State-selective charge exchange from Na(3s) and Na*(3p) by highly charged ions

2010 J. Phys. B: At. Mol. Opt. Phys. 43 155203

(http://iopscience.iop.org/0953-4075/43/15/155203)

J. Phys. B: At. Mol. Opt. Phys. **43** (2010) 155203 (8pp) doi:10.1088/0953-4075/43/15/155203

State-selective charge exchange from Na(3s) and Na*(3p) by highly charged ions

S Otranto[1] **and R E Olson**[2]

[1] CONICET and Departamento de Física, Universidad Nacional del Sur, 8000 Bahía Blanca, Argentina
[2] Physics Department, Missouri University of Science and Technology, Rolla, MO 65401, USA

E-mail: sotranto@uns.edu.ar and olson@mst.edu

Received 15 April 2010, in final form 14 June 2010
Published 7 July 2010
Online at stacks.iop.org/JPhysB/43/155203

Abstract
State-selective charge exchange cross sections and momentum spectra are calculated for collisions of Xe^{18+} and Xe^{54+} ions with Na(3s) and Na*(3p) over the energy range of 0.1–10.0 keV/amu. The classical trajectory Monte Carlo method is used which includes all two-body interactions. The n-level cross sections are found to be rather insensitive to collision energy below 1 keV/amu. In contrast, the transverse momentum cross sections for specific n-levels change rapidly with energy. However, this latter variation in energy is found to be in general agreement with simple scaling rules. Experimental state-selective data are available for Xe^{18+} over a limited energy range; they are found to be in reasonable accord with the calculations.

(Some figures in this article are in colour only in the electronic version)

Introduction

Multiply charged ion electron capture collisions have been investigated for many years. Starting in the 1970s, interest centred on collisions of multiply charged ions of C, N and O colliding with atomic hydrogen. The investigations were prompted by the tokamak fusion reactor program where photon emission after electron capture was used as a diagnostic for the impurity ion concentrations, the temperature and the rotation of the plasma. Collision energies of interest were 1–80 keV/amu. Energies less than 10 keV/amu coincided with the inherent temperatures and collisions in the plasmas, while higher energy cross sections were needed for spectroscopic studies made during neutral beam injection that was used for fuelling and heating the plasma [1].

More recently, renewed interest in multiply charged ion electron capture processes has been motivated by the observation of x-rays from comets [2–4]. Here, the collision processes mainly involved C, N, O and Ne ions from the solar wind colliding with the H_2O gas evaporated from the comet as it passes through our solar system. The energy range of interest is around 1 keV/u, slightly higher or lower depending on which solar wind component one is concerned with.

Now interest has shifted back to tokamak applications due to the planned construction of a large, international, high temperature tokamak fusion reactor (ITER) in Cadarache, France [5]. In order to extract power from such a reactor, one idea is to inject heavy rare gases into the divertor region. In this area it is expected that charge exchange by highly charged ions, followed by photon emission, will uniformly heat the divertor surfaces, thus, removing the risk of the plasma concentrating its heat on a localized region of the container walls. However, a small amount of data exist for high charge states of Ar or Xe colliding with H or D atoms. Moreover, it is well known that the metastable $H^*(n = 2)$ or $D^*(n = 2)$ atoms provide a very high fraction of the visible range photon flux even though they reside as only 1% of the ground state. This is because their cross sections are so much larger than those for the ground state [1].

So far, it has been experimentally infeasible to provide cross sections for $H^*(n = 2)$ targets to provide benchmark data to test theoretical methods. However, ground-state alkali atoms have very similar cross sections due to their nearness in ionization potentials. In a recent experimental breakthrough, there are now benchmark state-selective data available for Xe^{18+} ions colliding with Na(3s) measured using the MOTRIMS (magneto optical trap recoil ion momentum spectroscopy) method [6]. These studies complement previous analyses performed with the projectiles of lower charges (He^{2+} and C^{4+}) on Na(3s) and Na*(3p) by the same group [7, 8].

One purpose of this paper is to use the three-body classical trajectory Monte Carlo (CTMC) method to test it against the data for state-selective electron capture:

$$\begin{aligned} \mathrm{Xe}^{q+} + \mathrm{Na}(3s) &\rightarrow \mathrm{Xe}^{(q-1)+}(n) + \mathrm{Na}^{+}, \\ \mathrm{Xe}^{q+} + \mathrm{Na}^{*}(3p) &\rightarrow \mathrm{Xe}^{(q-1)+}(n) + \mathrm{Na}^{+}. \end{aligned} \tag{1}$$

For scaling purposes, we have extended the Xe^{18+} calculations, where data are available, to those for Xe^{54+}. Also, since all two-body interactions are included, we are able to provide momentum differential spectra and deduce scaling relationships. The $Na^*(3p)$ target is included in our study to provide guidance for future experimental studies. The energy range investigated is 0.1–10 keV/amu, and termed as intermediate since the collision speeds surround those of the target electron which corresponds to 9.4 keV/amu for Na(3s) and 5.6 keV/u for $Na^*(3p)$.

Theoretical method

We have performed CTMC calculations of the cross sections for single-electron capture [9]. Hamilton's equations were solved for a mutually interacting three-body system. The centre of mass of the Na target is frozen at the beginning of each simulation. The active electron evolves under the central potential model developed by Green *et al* from Hartree–Fock calculations [10], and later generalized by Garvey *et al* [11]. The CTMC method directly includes the ionization channel and is not limited by basis set size for the prediction of capture to very high lying excited states. The Na(3s) and $Na^*(3p)$ states are distinguished not only through their respective ionization potentials but also by means of the classical angular momentum restriction $l^2 < 1$ and $1 < l^2 < 4$, respectively [12].

Since the electron tends to be captured to high n-values with minimal contributions from the s-, p-, and d-states, quantum defects play a minor role and the orbital energies for the captured electron are similar to those obtained with bare projectiles. We then represent the captured electron–projectile interaction by a Coulomb potential where the projectile asymptotic charge is considered.

A classical number n_c is obtained from the binding energy E_p of the electron relative to the projectile by

$$E_p = -Z_p^2/(2n_c^2), \tag{2}$$

where Z_p is the charge of the projectile core. Then, n_c is related to the quantum number n of the final state by the condition derived by Becker and McKellar [13]:

$$[(n-1)(n-1/2)n]^{1/3} \leqslant n_c \leqslant [n(n+1)(n+1/2)]^{1/3}. \tag{3}$$

The cross section for a definite n-state is then given by

$$\sigma_n = N(n)\pi b_{\max}^2/N_{\mathrm{tot}}, \tag{4}$$

where $N(n)$ is the number of events of electron capture to the n-level and N_{tot} is the total number of trajectories integrated. The impact parameter $b_{\max}$ is the value beyond which the probability of electron capture is negligibly small.

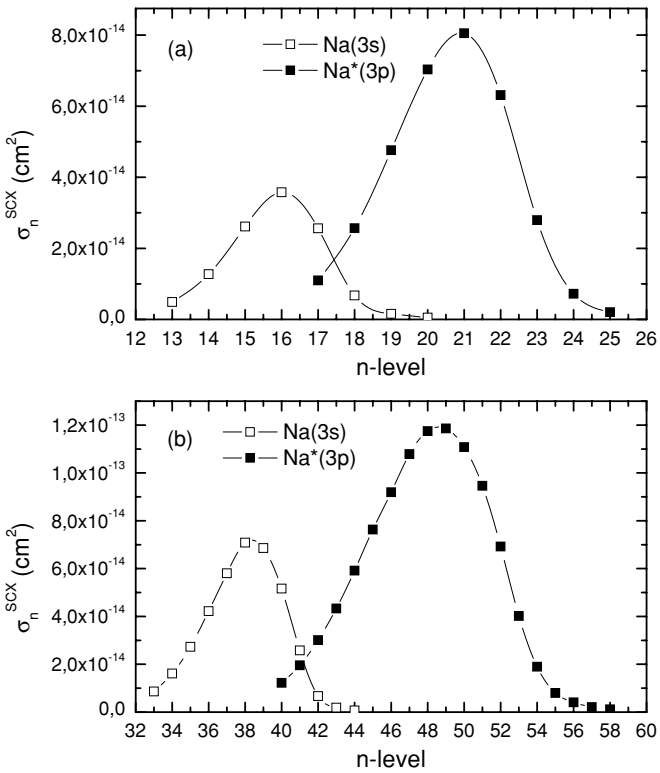

Figure 1. State-selective electron capture cross sections for 1 keV/amu collisions on Na(3s) and $Na^*(3p)$ targets by (a) Xe^{18+}; (b) Xe^{54+} ions.

Results

In figure 1 we display 1 keV/amu state-selective cross sections for the four systems under study in this paper. The results are presented in a format that illustrates the significant shift to a higher principal quantum number that arises from optically pumping the ground Na(3s) to its first excited $Na^*(3p)$ state. Note also that the $Na^*(3p)$ cross sections are significantly larger than those for the ground state due to the lower ionization potential and larger radial extension for $Na^*(3p)$ versus Na(3s).

Some time ago, it was predicted that the peak in the n-selective cross sections should maximize at

$$n_p = n_i \times q^{3/4} = (13.6\ \mathrm{eV/IP})^{1/2} q^{3/4}, \tag{5}$$

where n_i is related to the ionization potential IP using simple hydrogenic scaling laws [12]. More recently, calculations on the Li target for charge states up to 10+ showed that a prefactor of approximately 1.2 is needed to account for the non-hydrogenic potential that the electron is subject to in its initial state [14]. If we fit the results of the calculations presented in figure 1, we also find for both Na(3s) and $Na^*(3p)$ targets

$$n_p \approx 1.2 \times (13.6\ \mathrm{eV/IP})^{1/2} q^{3/4}. \tag{6}$$

Indeed, the early predictions of a $q^{3/4}$ dependence are still supported. We note that there is a slight energy dependence to this scaling, which will be seen in the next several figures. The magnitude of the principal quantum numbers populated after electron capture may seem excessively large, but one must

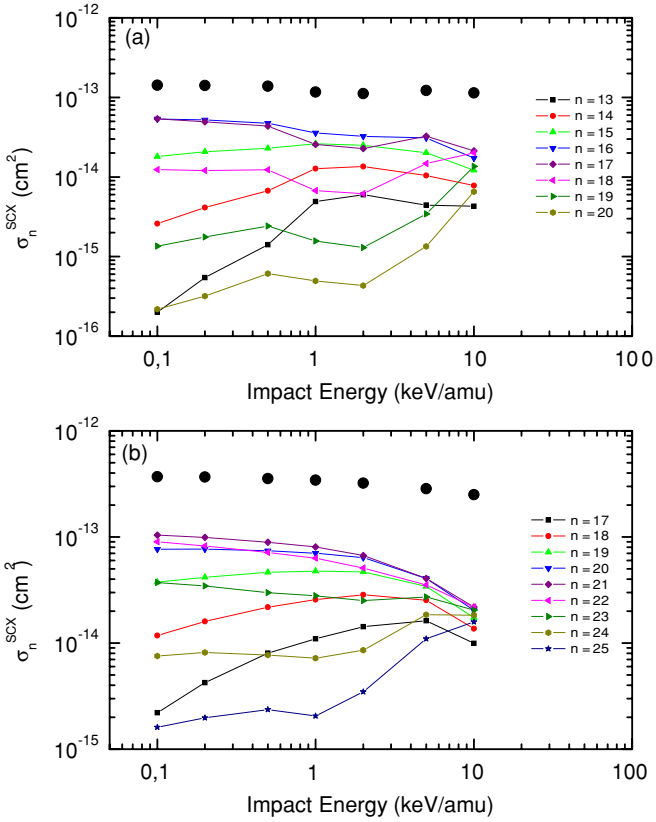

Figure 2. *n*-state-selective capture cross sections for Na(3s) and Na*(3p) targets as a function of collision energy for Xe^{18+}. For reference, the solid circles are the total charge exchange cross sections.

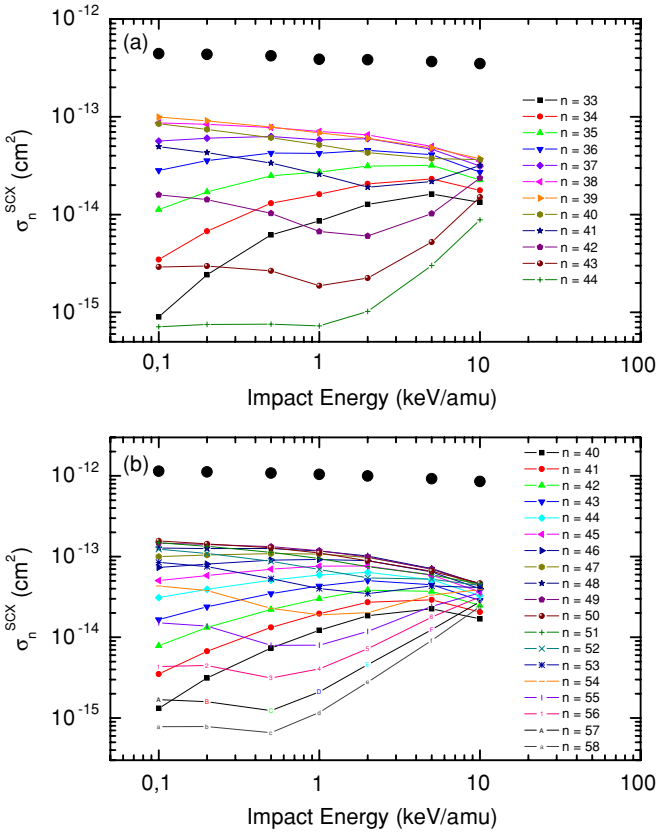

Figure 3. *n*-state-selective capture cross sections for Na(3s) and Na*(3p) targets as a function of collision energy for Xe^{54+}. For reference, the solid circles are the total charge exchange cross sections.

remember that these reactions are exoergic and the final states are still more tightly bound than the initial state.

In figures 2 and 3 the *n*-selective capture cross sections for Na(3s) and Na(3p) targets are presented as a function of the collision energy for the Xe^{18+} and Xe^{54+} systems, respectively. The overall total charge exchange cross sections are given by the solid circles. At 1 keV/amu the total charge exchange cross sections for both targets under consideration scale as

$$\sigma_{\mathrm{SCX}} \propto q. \tag{7}$$

As previously predicted, the total electron capture cross sections are approximately linear in the charge state [15]. For 1 keV/amu collisions with charge states from 8+ to 92+, the proportionality factor for equation (7) is 7.0×10^{-15} cm^2 and 1.9×10^{-14} cm^2 for the ground- and excited-state targets, respectively. Note that the Na*(3p) total charge exchange cross sections are approximately a factor of 3 larger than those for the ground state. In all cases the total charge exchange cross sections decrease at the higher energies because of the increasing importance of the ionization channel that removes flux from the capture component. One can see that the capture process is sharply peaked in *n*-value at the lowest energy leading to large cross sections for only a few *n*-values. However, at the highest energy the *n*-distribution is considerably broadened due to strong mixing of the capture channels in the increasingly important small impact parameter collisions.

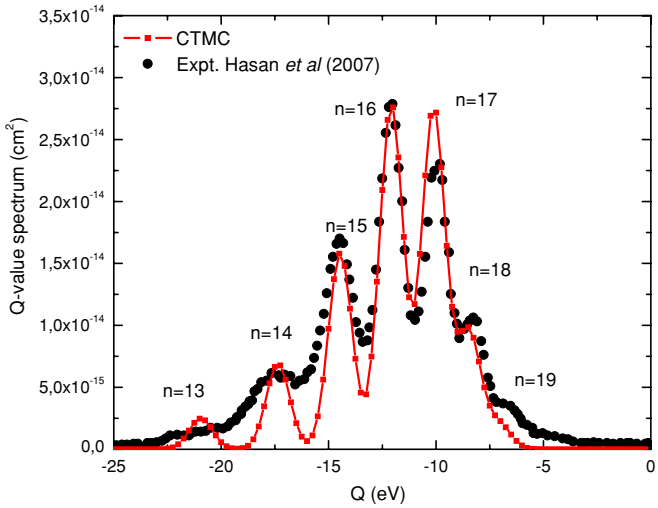

Figure 4. Energy gain (Q-value) spectrum for 2.23 keV/amu Xe^{18+} on Na(3s). The experimental data shown are those from Hasan *et al* [6].

The theoretical cross sections presented for Xe^{18+} on Na(3s), figure 2, can be compared to experimental data obtained by the Gröningen experimental group led by Hoekstra. The measurements were obtained using the newly developed MOTRIMS method [6]. In figure 4 the experimental data for the energy gain, Q-value, in the Xe^{18+} on Na(3s)

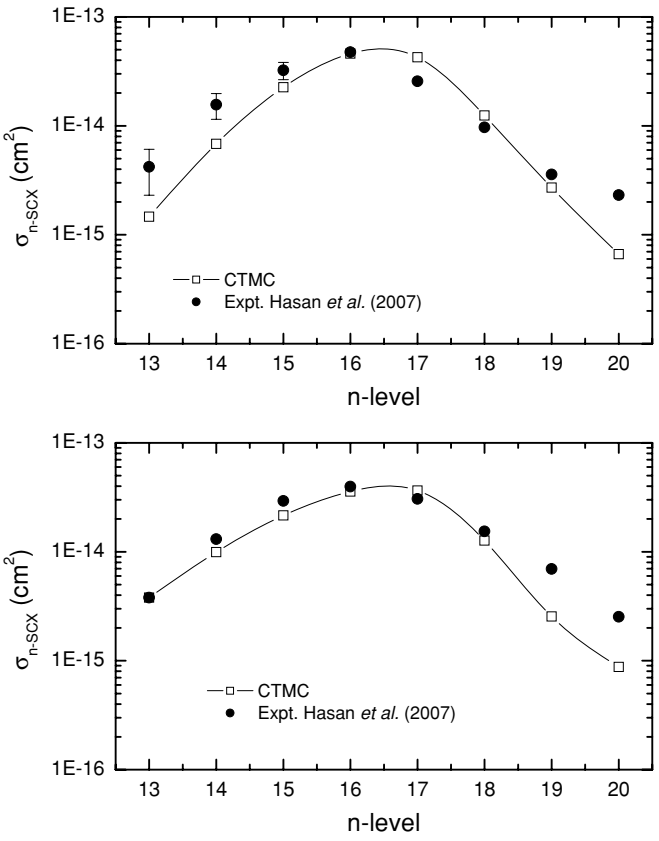

Figure 5. n-state-selective capture cross sections for 0.55 and 3.35 keV/amu Xe^{18+} collisions on Na(3s). The experimental data shown are from [6].

collision at 2.23 keV/amu are shown. We have convoluted our calculations for the n-spectra using a Gaussian FWHM energy width of 1.3 eV. This is consistent with an experimental energy resolution that was stated to be 1–2 eV. Overall, there is good agreement between theory and experiment except maybe for the lowest n-values. For these cases the detector extraction fields produce a double-peak structure that is not simulated in our theoretical calculations.

In figure 5 a comparison between theory and experiment at the lowest, 0.55 keV/amu, and highest, 3.35 keV/amu, energies accessible to the measurements are shown. The major discrepancy appears for the highest n-values where theory tends to underestimate the cross sections implying that the cross sections arising from large impact parameters may be underestimated. However, the magnitudes for these latter values are an order of magnitude smaller than the peak values, meaning they are a minor component of the overall total charge exchange cross section. We must also emphasize that in figures 4 and 5 we have normalized the experimental data to our cross sections in the peak region because the experimental data are relative, not absolute in magnitude.

Since all two-body interactions are included in the CTMC calculations, it is possible to predict the behaviour of the recoil transverse momentum cross sections differential in the product n-level. These cross sections shift rapidly in collision energy, as one would expect from a simple calculation of the transverse impulse for a Coulomb interaction between two charges Z_1 and Z_2:

$$p_{\text{trans}} = \alpha \frac{Z_1 Z_2}{bv}, \tag{8}$$

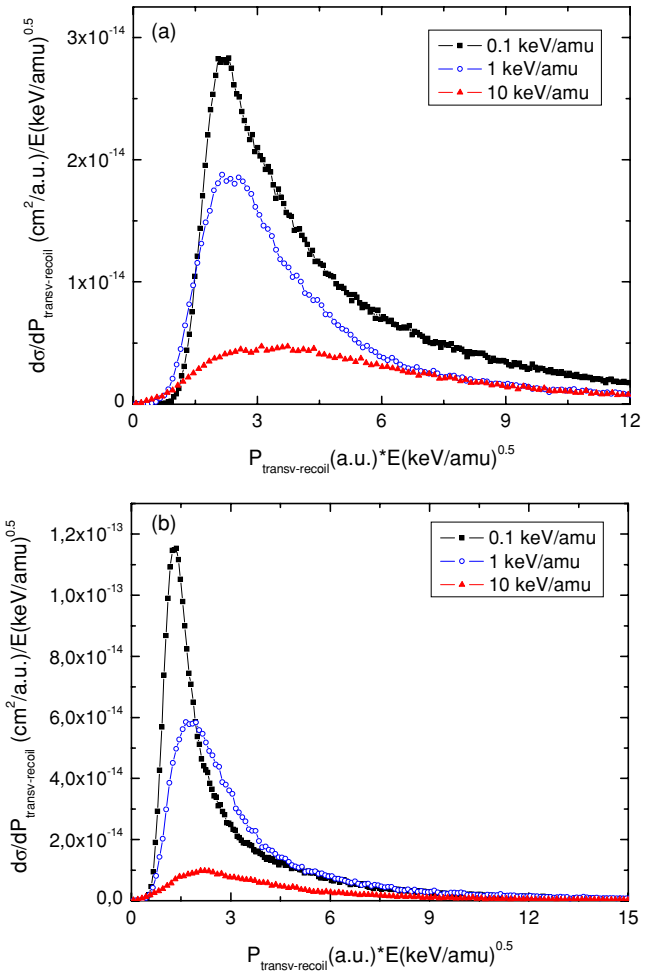

Figure 6. Recoil ion transverse momentum spectrum for 0.1, 1 and 10 keV/amu Xe^{18+}collisions on (a) Na(3s) target (capture to $n = 16$) and (b) Na^*(3p) target (capture to $n = 21$).

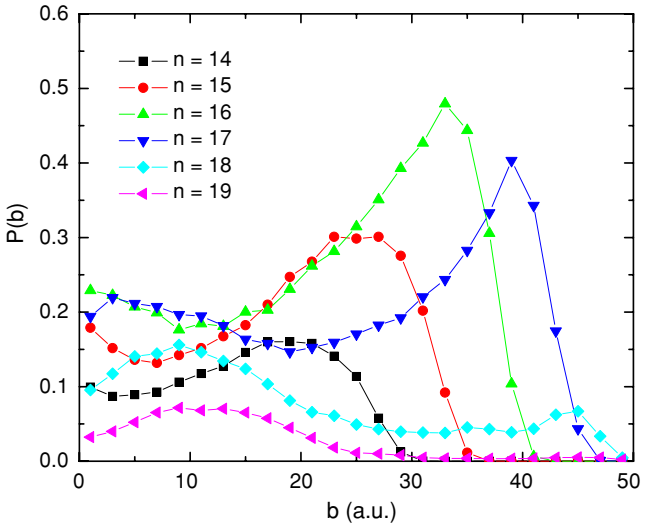

Figure 7. Electron capture transition probabilities as a function of the product n-level for 1 keV/amu Xe^{18+} collisions on Na(3s).

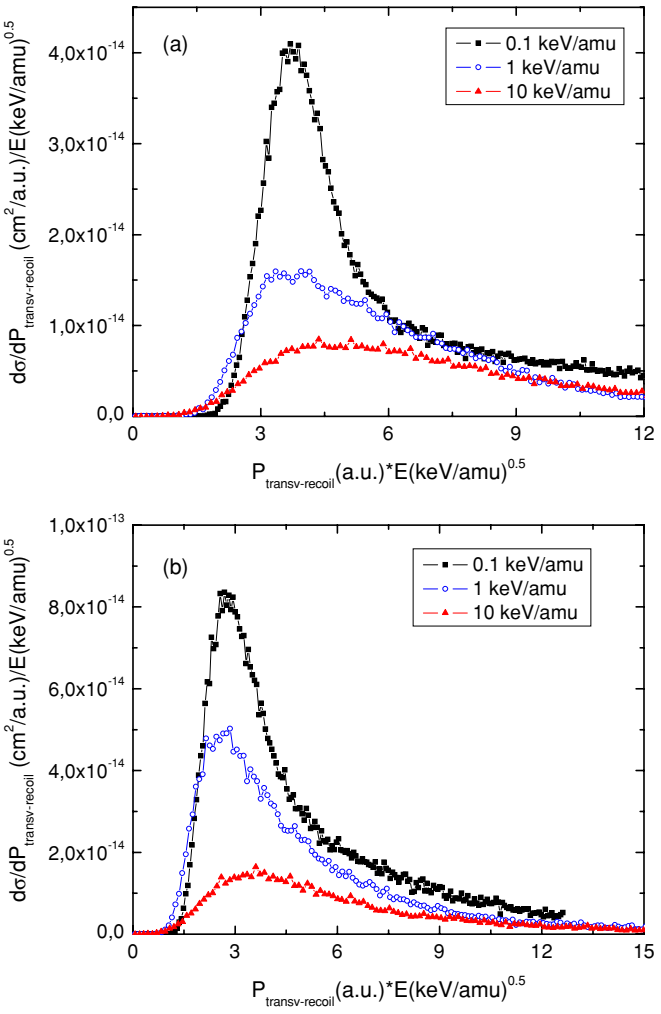

Figure 8. Recoil ion transverse momentum spectrum for 0.1, 1 and 10 keV/amu Xe^{54+} on (a) Na(3s) collisions (capture to $n = 39$) and (b) $Na^*(3p)$ collision (capture to $n = 50$).

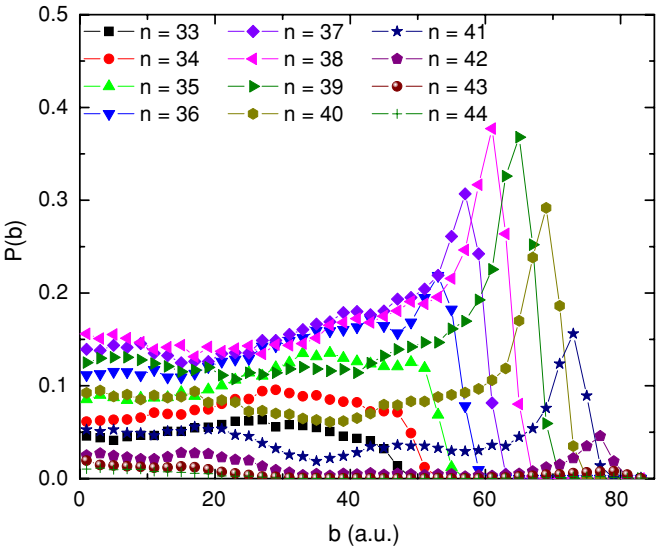

Figure 9. Electron capture transition probabilities as a function of the product n-level for 1 keV/amu Xe^{54+} on Na(3s) collisions.

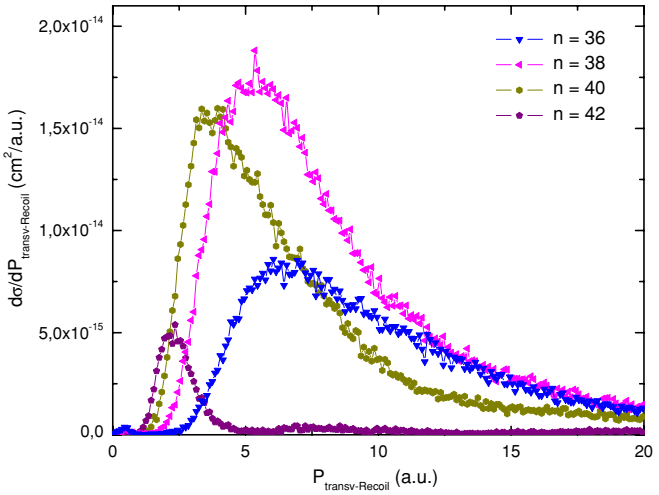

Figure 10. Recoil ion transverse momentum spectrum for 1 keV/amu Xe^{54+} collisions on Na(3s) target for product n-levels 36, 38, 40 and 42.

where α is equal to 2, and v is the collision speed and b is the impact parameter. Thus, a plot using $E^{1/2} \times p_{\text{trans}}$ as the abscissa should remove much of the energy dependence since the impact parameter dependence of the cross sections changes very slowly with energy. Furthermore, a linear scale can be preserved if the corresponding ordinate of the cross section differential in transverse momentum is divided by $E^{1/2}$.

In figure 6 0.1, 1 and 10 keV/amu Xe^{18+} results for the Na(3s) target and the $n = 16$ product state and $Na^*(3p)$ for the $n = 21$ state are shown. As expected, the $Na^*(3p)$ cross sections peak at smaller values of p_{trans} than Na(3s) due to the larger range of interaction. To make a qualitative test of equation (8), let us specifically examine more closely the 1 keV/u Na(3s) results. The p_{trans} cross sections maximize at around 2.5 on the $E^{1/2} \times p_{\text{trans}}$scale. Now, in figure 7 we display the electron capture transition probabilities for 1 keV/amu Xe^{18+} on Na(3s) collisions as a function of the product n-level. Note that the $n = 16$ transition probability maximizes at about 33 au. Using equation (8) above, we find that α is essentially equal to unity, yielding the relationship between the p_{trans} cross sections and the impact parameter of

$$p_{\text{trans}} = \frac{(q-1)}{bv} \tag{9}$$

for single-electron capture with the target singly ionized. In hindsight, a value of α equal to unity should be expected since the interaction only follows a Coulomb trajectory for half the collision which is the outward portion, while the incoming portion is controlled by a more benign point-charge induced dipole interaction. Furthermore, for qualitative purposes, the use of equation (9), measured p_{trans} data, and the Coulomb cross sections can in the future be used to roughly describe the transition probabilities as a function of impact parameter.

To further test equation (9), in figure 8 the cross sections differential in transverse momenta for the $n = 39$ and $n = 50$ product levels for Xe^{54+} colliding with Na(3s) and $Na^*(3p)$

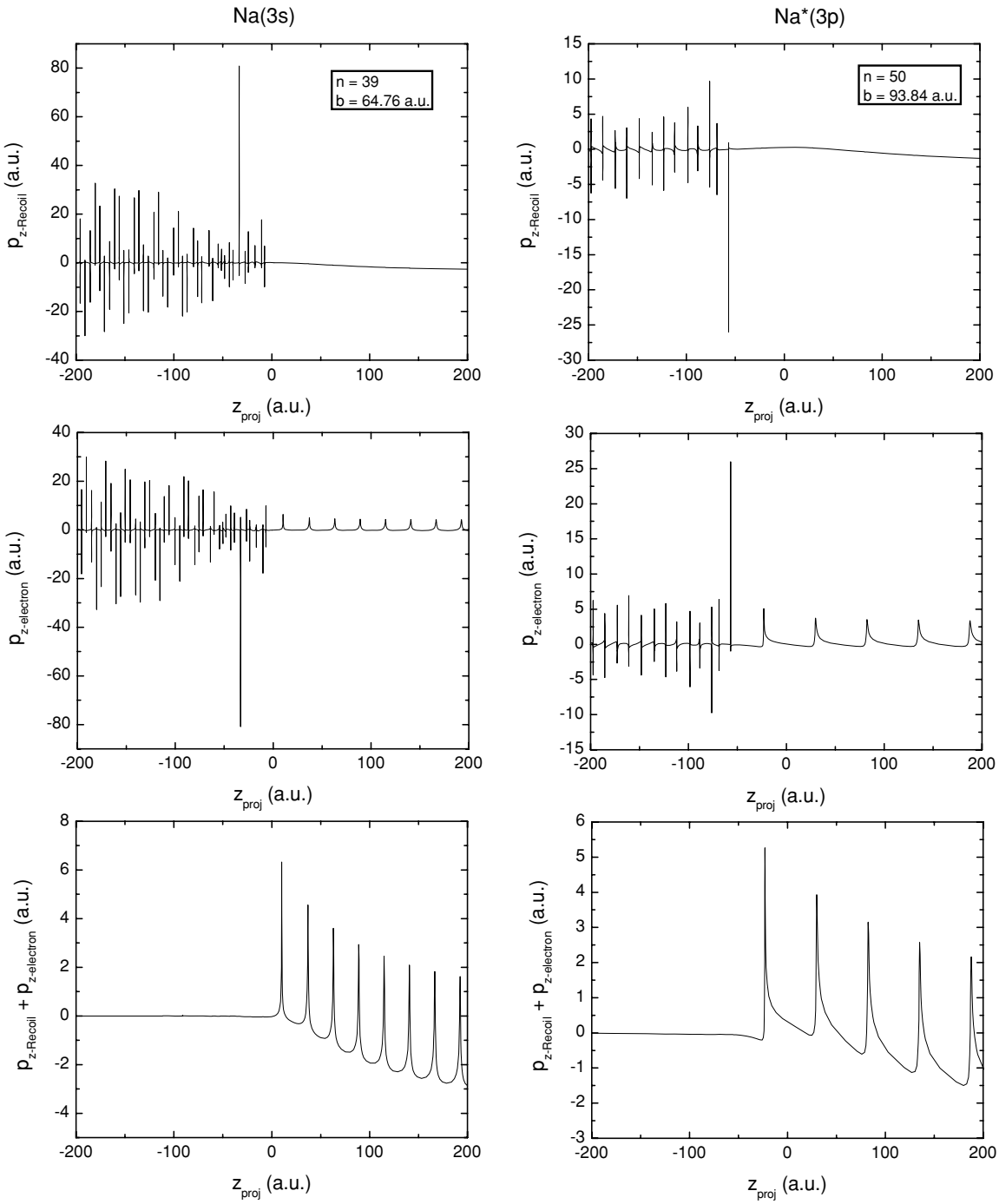

Figure 11. Recoil, electron and total recoil + electron p_z components as a function of $z_{\rm proj}$ for a typical trajectory leading to capture to (left column) $n = 39$ in 1 keV/amu Xe^{54+} collisions on Na(3s) and (right column $n = 50$ in 1 keV/amu Xe^{54+} collisions on Na*(3p).

at 0.1, 1 and 10 keV/amu, respectively, are displayed. As in the Xe^{18+} systems, the Na*(3p) cross sections peak at smaller values of $p_{\rm trans}$ than for the ground state. This is just a reflection of the longer range of the interactions for the loosely bound excited state. In both cases, the n-levels were chosen to be near the maximum value for the states selective cross sections.

The range of interaction for the Xe^{54+} systems is quite large and extends to 100 au and 150 au for Na(3s) and Na*(3p), respectively. Examining the Na(3s) system in figure 8, we find that the 1 keV/amu differential cross section maximizes near a transverse momentum of 3.75 au. Using equation (9), one would predict that the transition probability for $n = 39$ will maximize close to an impact parameter of 71 au. In figure 9 the 1 keV/amu transition probabilities are given for Xe^{54+} on Na(3s) collisions. We see that the $n = 39$ product state has a maximum at about 65 au near the predicted value using equation (9) and the transverse momentum cross section.

Also of interest in figure 9 is the progression for the largest n-values to peak at the largest impact parameters with the

maximum values arising in the 60–65 au range. Note also how below 40 au all the n-value transition probabilities are relatively constant, indicating a complex mixing between the states on the repulsive wall of the collision. Such behaviour is not predicted by analytical over-the-barrier models [16].

So far we have only displayed the transverse momentum spectra for one n-value for each collision system. It is worth illustrating how these cross sections change with the product state. From equation (9) we find an inverse relation between impact parameter and transverse momentum. This is born out very well in figure 10 where 1 keV/amu results for Xe^{54+} on Na(3s) are displayed. Referring back to the transition probabilities given in figure 9, we find a progression for the large n-values to peak at the small transverse momentum values and vice versa.

We could show any number of individual trajectories for the collisions studied above. However, there are some general characteristics that can be illustrated in one figure. We chose a trajectory from a 1 keV/amu collision of Xe^{54+} on Na(3s) and Na^*(3p) for the impact parameters of 64.76 au and 93.84 au, respectively. The product capture states are $n = 39$ and $n = 50$, figure 11. In all cases the z-components of the momenta are presented.

First, on the incoming portion of the trajectory, one can see the z-component of the Compton profile of the electron as it orbits about the Na^+ core—first row for both targets (note that the momentum values are large due to the non-hydrogenic model potential used in the initial state description of Na). In the second row one then finds that the Na^+ core possesses an out-of-phase Compton profile so that the total atom, as in the experiments, is 'frozen' with zero momentum (third row).

We now describe the main trends that can be inferred for the Na(3s) target from the typical trajectory. The strong peak exhibited by the recoil at $z_{\rm proj} = -33$ au clearly indicates that the capture process begins before the distance of closest approach. For such a slow, asymmetric collision system, the electron is highly polarized and is quickly captured by the projectile. In the middle figure ($p_{z\text{-electron}}$ vs $z_{\rm proj}$) one can see the uniform oscillations of the electron after capture in the out-going portion of the trajectory.

With respect to the Na^*(3p) target, we first note that the momentum values for the unperturbed atom now oscillate with a minor amplitude possibly due to the $1 < l^2 < 4$ restriction which prevents the electron orbit from getting close to the Na^+ parent ion. The collision process starts at about $z_{\rm proj} = -76$ au when the recoil is pushed forward by the Coulomb repulsion between the ionic centres. The electron orbit is strongly modified and now ends up close to the Na^+ ion with both the recoil and electron exhibiting large momentum values for $z_{\rm proj} = -56.8$ au. In this case we observe that the overall target does not remain frozen until the distance of closest approach. Instead, we observe that the target momentum drastically changes while the projectile is still approaching (note the peak at $z_{\rm proj} = -22$ au). It is important to note that for some trajectories we have observed that the electron is not simply captured and carried away by the projectile, but orbits about both ion centres in a very complex manner.

Conclusions

In this work we have studied state-selective charge exchange processes for the collisions of Xe^{18+} and Xe^{54+} ions with Na(3s) and Na^*(3p) over the energy range of 0.1–10.0 keV/amu. In particular, CTMC state-selective charge exchange cross sections and momentum spectra were presented. We found, as expected, that capture cross sections from Na^*(3p) are larger than those from Na(3s). Furthermore, they populate larger n-values of the projectile at the same collision energy. We note that simple trends derived decades ago, like the $q^{3/4}$ dependence for the most probable n-level for capture, are still valid. However this simple scaling rule was derived for hydrogenic targets, and for the present case predicts n_p values which are too low by about 20%. The discrepancy is probably due to the non-Coulomb part of the active electron–target interaction. More work is needed in order to determine which parameters (IP, atom size etc) are important in estimating the n_p value for non-hydrogenic targets.

We have compared our theoretical predictions for the n-state-selective capture cross sections with available relative experimental data for Xe^{18+} + Na(3s) from the Gröningen group led by Hoekstra. Within the impact energy range, experimentally explored, we found that our calculations are in reasonable agreement with the data.

Finally, from the obtained results for the recoil $p_{\rm trans}$ distributions, we have presented, based on physical grounds, a simple relation to approximately determine the impact parameters at which those distributions are expected to peak.

Since these highly charged ion collision systems are still hard to calculate using state-of-the-art numerically intensive quantum-mechanical methods, the present results show that the CTMC method provides a fast and confident platform for these studies. It is also worth noting that a Li MOT has recently been included in a reaction microscope allowing photo-double ionization studies on Li(1s2nl) [17, 18]. Future measurements are also planned at GSI-Darmstadt which will eventually test our predictions.

Acknowledgments

Work at UNS supported by PGI 24/F049, PICT-2007-00887 of the ANPCyT and PIP 112-200801-02760 of CONICET (Argentina).

References

[1] Isler R C 1994 *Plasma Phys. Control. Fusion* **36** 171
[2] Cravens T E 1997 *Geophys. Res. Lett.* **24** 105
[3] Beiersdorfer P *et al* 2003 *Science* **300** 1558
[4] Otranto S, Olson R E and Beiersdorfer P 2006 *Phys. Rev.* A **73** 022723
[5] www.iter.org
[6] Hasan V G, Knoop S, Morgenstern R and Hoekstra R 2007 *J. Phys. Conf. Ser.* **58** 199
[7] Schippers S, Boduch P, van Buchem J, Bliek F W, Hoekstra R, Morgenstern R and Olson R E 1995 *J. Phys. B: At. Mol. Opt. Phys.* **28** 3271

[8] Schippers S, Hoekstra R, Morgenstern R and Olson R E 1996 *J. Phys. B: At. Mol. Opt. Phys.* **29** 2819
[9] Olson R E and Salop A 1977 *Phys. Rev.* A **16** 531
[10] Green A E S, Sellin D L and Zachor A S 1969 *Phys. Rev.* **184** 1
[11] Garvey R H, Jackman C H and Green A E S 1975 *Phys. Rev.* A **12** 1144
[12] Olson R E 1981 *Phys. Rev.* A **24** 1726
[13] Becker R L and McKellar A D 1984 *J. Phys. B: At. Mol. Phys.* **17** 3923
[14] Cornelius K R, Wojtkowski K and Olson R E 2000 *J. Phys. B: At. Mol. Opt. Phys.* **33** 2017
[15] Olson R E, Berkner K H, Graham W G, Pyle R V, Schlachter A S and Stearns J W 1978 *Phys. Rev. Lett.* **41** 163
[16] Niehaus A 1986 *J. Phys. B: At. Mol. Phys.* **19** 2925
[17] Steinmann J 2007 *20th Int. Symp. on Ion Atom Collisions 2007 (Agios Nikolaos, Crete, Greece)* Invited talk at
[18] Zhu G, Schuricke M, Steinmann J, Albrecht J, Ullrich J, Ben-Itzhak I, Zouros T J M, Colgan J, Pindzola M S and Dorn A 2009 *Phys. Rev. Lett.* **103** 103008